Optics Letters

Brillouin instantaneous frequency measurement with an arbitrary response for potential real-time implementation

Weiwen Zou,* Xin Long, Xing Li, Guangyao Xin, and Jianping Chen

State Key Laboratory of Advanced Optical Communication Systems and Networks, Intelligent Microwave Lightwave Integration Innovation Center (iMLic), Department of Electronic Engineering, Shanghai Jiao Tong University, Shanghai 200240, China
**Corresponding author: wzou@sjtu.edu.cn*

Received 14 January 2019; revised 19 February 2019; accepted 21 February 2019; posted 25 March 2019 (Doc. ID 357563); published 10 April 2019

We demonstrate an arbitrary-response Brillouin instantaneous frequency measurement (IFM) based on the principle of the frequency-to-power mapping in stimulated Brillouin scattering (SBS), which is named Brillouin IFM. The arbitrary response is realized by periodically sweeping the frequency of the local pump lightwave, and the response's amplitude depends on the sweeping slope. The Brillouin IFM is achieved by the control of the sweeping period lower than the double of the flight-of-time in the SBS interaction length. A Costas frequency coded pulse is experimentally measured to verify the feasibility of the proposed Brillouin IFM scheme. The bandwidth of the digital sampling in the scheme is reduced to 50 MHz. The Brillouin IFM range without averaging reaches 6 GHz at Ku band.

https://doi.org/10.1364/OL.44.002045

Instantaneous frequency measurement (IFM) is an important technique to directly identify the frequency of an unknown microwave signal without complicated digital processing. It ensures a fast response for electronic reconnaissance and warfare [1]. In the last decades, several photonics-assisted IFM schemes [2–7] are raised to provide a broadband measurement range, which are usually implemented by using wideband quadrature hybrid couplers and delay lines similar to the traditional electronic IFM receivers [8,9]. The principles of these schemes can be mainly classified as the frequency-to-power mapping [2–6] or frequency-to-time mapping [7]. The former one is more commonly used by simply designing a monotonous system response, or so-called the amplitude comparison function (ACF). It can be achieved by optical delay lines [10], dispersion [7], and other nonlinear phenomena [5,6]. However, most ACFs of these schemes are limited by the specific parameters of the photonic devices (such as optical fiber length). Some schemes might program the system's ACF by tuning the wavelength of the light source [4,5], but it is still difficult to achieve an arbitrary response.

The stimulated Brillouin scattering (SBS) process is a nonlinear phenomenon of three-wave interaction involving the pump lightwave, counter-propagating probe lightwave, and acoustic wave [11]. It occurs when the beat frequency between the pump and probe lightwaves is close enough to the Brillouin frequency shift (BFS) of the SBS interaction media. According to the nature of phonon-photon interaction, SBS has been studied and used for many signal processing applications [12–20]. For the IFM application, SBS is expected to provide high-frequency resolution for its narrow-bandwidth filtering feature. In Ref. [19], an SBS-based IFM was proposed based on the dependence of the BFS on the optical wavelength. However, this scheme can only measure high frequency (>20 GHz), because the observation of the BFS change requires a large wavelength difference. Besides, an SBS-based IFM has been successfully implemented in a chip-scale device, and both large measurement range and high resolution are simultaneously achieved [5]. However, the frequency of the signal to be detected should be constant or composed of several tones. Most recently, we have realized the measurement of the instantaneous spectrum of an unknown microwave signal via SBS [6]. However, the real-time detection is hardly achievable due to the requirement of the repeatability of the signal and the frequency tuning process.

In this Letter, we present a Brillouin IFM scheme with an arbitrary response, which provides a potential solution for real-time implementation. The unknown signal is modulated onto the probe lightwave, and the pump lightwave is modulated by a designed frequency sweeping signal. The instantaneous spectrum is converted by the frequency-to-power mapping principle and obtained by detecting the Brillouin gain. Through periodically sweeping the frequency of the pump lightwave, the broadband measurement range is achieved, and an arbitrary response is realized by controlling the sweeping slope. An experiment in a 2.6 km dispersion compensate fiber (DCF) is carried out to measure the frequency Costas coded pulse [20]. The Brillouin IFM detection without averaging is demonstrated with the instantaneous bandwidth of 6 GHz at Ku band.

The system response $\boldsymbol{H}(\omega)$ of an SBS pump-probe-based configuration is exactly the intrinsic Brillouin gain spectrum (BGS) when the continuous pump lightwave has a constant frequency of ω_P [11]:

$$\boldsymbol{H}(\omega)=\frac{\boldsymbol{G}(\omega)}{\boldsymbol{E}_S(\omega)}\propto\frac{g_0}{1/(2\tau_p)+i(\omega-\omega_P+\omega_B)}, \quad (1)$$

where $\boldsymbol{G}$ and $\boldsymbol{E}_S$ represent the spectrum of the slowly-varying envelopes of Brillouin gain and injected probe lightwaves, respectively. g_0 is the Brillouin gain coefficient, and τ_p stands for the phonon lifetime. $\omega_B/2\pi$ is the BFS of the SBS interaction media. By tuning ω_P and detecting the probe gain, one can locate all frequency components under the Bragg condition of $\omega_P-\omega_B$. As the SBS response is narrow due to the phonon lifetime (~10 ns), the frequency of the pump lightwave has to be tuned step by step for the wideband measurement [6,17], which is not possible for single-shot detection.

To realize an arbitrary-response Brillouin IFM for potential real-time implementation, the broadband system response is essentially required for single-shot measurement. The system response $\boldsymbol{H}(\omega)$ of the SBS-based IFM can be regarded as the convolution result between the pump spectrum $\boldsymbol{E}_P(\omega)$ and the intrinsic BGS $\boldsymbol{G}_0(\omega)$:

$$\boldsymbol{H}(\omega)\propto\boldsymbol{G}_0(\omega)\otimes\boldsymbol{E}_P(\omega). \quad (2)$$

In principle, one can utilize a linear or nonlinear frequency sweeping to the pump lightwave to broaden $\boldsymbol{H}(\omega)$. As illustrated in Fig. 1, they have different system responses from those with no sweeping to the pump lightwave. For a constant frequency of the pump lightwave, the system response keeps narrow as the intrinsic BGS, which is illustrated in Fig. 1(a). With the frequency sweeping (green curves), the local BGSs (blue and red curves) are frequency shifted along the SBS interaction media, resulting in a wideband response (black dashed curves). However, different sweeping slopes may cause different response shapes. As shown in Fig. 1(b), the system response is relatively flat, because the frequency sweeping is linear; thus, every frequency component contributes equally to the final $\boldsymbol{H}(\omega)$. In an IFM scheme, and a monotonous response with a large slope is required to provide high-frequency resolution. This can be achieved through nonlinear frequency sweeping [see Fig. 1(c)]. As the frequencies are swept with different slopes, the local BGSs are nonuniformly distributed along the SBS interaction media, and the final system response is more possible for potential real-time IFM implementation.

According to Eq. (2), when the pump lightwave is a broadband signal beyond GHz, the intrinsic BGS can be regarded as an impulse function, because its bandwidth is usually considered as 50 MHz in a silica optical fiber [11,13]. In this situation, $\boldsymbol{H}(\omega)$ is dependent on the designed pump lightwave's spectrum $\boldsymbol{E}_P(\omega)$. Note that the sweeping waveform is not the only choice to establish a broadband response. In principle, the amplitude of $\boldsymbol{E}_P(\omega_0)$ is relative to the time duration of a certain frequency ω_0. Longer time duration results in more Brillouin gain accumulated and stronger amplitude of the final response.

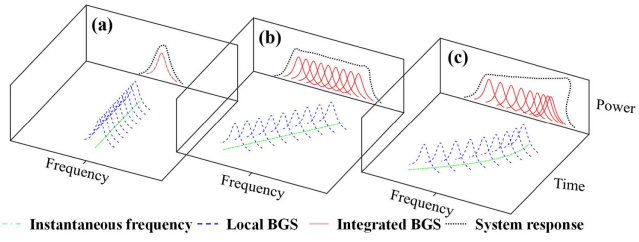

Fig. 1. Illustration of system responses for different pump lightwaves with (a) constant frequency, (b) linear frequency sweeping, and (c) nonlinear frequency sweeping.

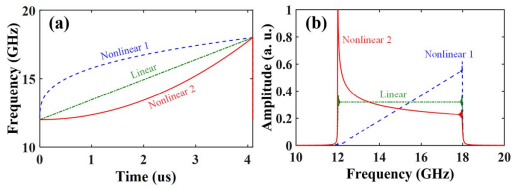

Fig. 2. Simulations for three frequency sweeping signals. (a) Instantaneous frequencies and (b) frequency spectrum.

Figure 2 shows the simulated system responses of three frequency sweeping signals (including linear and nonlinear sweeping) with different sweeping slopes. All three pump signals are swept from 12 to 18 GHz within 1 μs [see Fig. 2(a)]. Figure 2(b) shows their spectra of $\boldsymbol{E}_P(\omega)$. For a linearly frequency sweeping signal, which has the constant sweeping slope, the spectrum turns out to be a flat response [see the green curve in Fig. 2(b)]. When the frequency is swept nonlinearly, each frequency component lasts for a different time, resulting in a different response amplitude. Furthermore, a rising/falling response can be achieved by a nonlinearly frequency sweeping signal with a greater sweeping slope for higher/lower frequency [see blue and red curves in Fig. 2(b)]. It can be found that the nonlinear frequency sweeping instead of the linear frequency sweeping can achieve an IFM required system response.

To potentially implement the real-time Brillouin IFM, there are three more issues to be considered. One is the relationship between the length of the SBS interaction media (L) and the pump signal's sweeping duration (T_P). The Brillouin IFM receiver is always designed to detect unknown single-shot signals without prior knowledge of the arrival time. Therefore, the local pump lightwave's signal has to be periodically repeated during the IFM to catch the unknown single-shot signals. In this situation, T_P should be shorter than the double of the flight-of-time in the SBS interaction length to make sure that the pump and probe lightwaves can successfully meet each other, and SBS occurs within the SBS interaction media:

$$T_P\le\frac{2L}{v}, \quad (3)$$

where v is the light speed in the SBS interaction media. It should be noted that $2L/v$ also represents the maximum time of the pump lightwave that the probe lightwave can meet within the SBS interaction media. It is noted that the probe lightwave meets several periods of pump lightwave if T_P is pretty short. Consequently, there are ripples in the final response of $\boldsymbol{H}(\omega)$, which breaks the monotonicity of the designed response. In addition, the minimum measurement period of this scheme is L/v (around several microseconds). Note that the measurement period of our previous work [6] is at least several milliseconds due to the requirement of repeatable frequency tuning.

The second issue is the trade-off between the measurement range and resolution, which are two key performances of an IFM scheme. For a basic IFM based on the frequency-to-power mapping, the frequency information is converted into the amplitude information. Thus, these two performances, in fact,

are limited by the amplitude detection performance of the measurement system. Given the specific sampling and quantization module, the measured frequency resolution can be improved by enhancing the Brillouin gain. As it can be found in Eq. (1), a simple and effective way to enhance the Brillouin gain and improve the SNR is to utilize an SBS interaction media with high g_0 [20].

The last issue is the bandwidth needed for the photodetector (PD) and quantization module (i.e., analog-to-digital converter [ADC]) to implement the proposed Brillouin IFM. Since the frequency information is converted to the amplitude information after SBS, the PD and ADC only have to detect the probe gain, rather than the probe signal itself. Usually, the bandwidth of the probe gain is limited by the linewidth of the BGS or the inverse of the lifetime of the phonon and, therefore, is less than about 50 MHz in a silica optical fiber. Consequently, no matter what the carrier frequency or the signal's instantaneous bandwidth, the bandwidths of the PD and ADC just have to be less than 50 MHz in the proposed IFM scheme. Figure 3(a) depicts the experimental setup. A 1550 nm distributed-feedback laser (DFB-LD, NEL NLK1C6DAAA) is used as the light source and split into two branches by a 1:1 fiber coupler. The upper branch is modulated by a nonlinear frequency sweeping signal of an arbitrary waveform generator (AWG, Keysight M8152A) via a single-sideband modulator (SSBM) and works as the pump lightwave to form the specific system response. The lower branch, working as the probe lightwave, is modulated via a Mach–Zehnder modulator (MZM) by an unknown signal to be measured or a known linear frequency modulated (LFM) pulse signal for the IFM implementation or ACF characterization, respectively. Both erbium-doped fiber amplifiers (EDFA1 and EDFA2) are used to compensate for and control the optical power before launched into the SBS interaction media (such as an optical fiber). Polarization controllers (PC1 and PC2) are used to optimize the light polarizations before the SSBM and MZM, respectively. The injected powers of pump and probe lightwaves into the fiber are around 23 and 20 dBm, respectively. PC3 and PC4 ensure the maximum SBS interaction in a

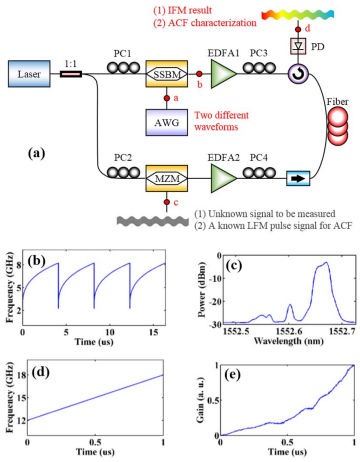

Fig. 3. (a) Experimental setup of the Brillouin IFM for ACF characterization of a known LFM pulse and for implementation of an unknown signal to be measured under two different pump lighwaves. (b) Instantaneous frequency of the pump lightwave. (c) Optical spectrum of the modulated pump lightwave. (d) Instantaneous frequency of the probe lightwave and (e) its Brillouin gain.

2.6 km DCF [20] with the BFS of ~9.76 GHz at 1550 nm. A circulator is used for the isolation and transmission of the amplified probe lightwave. A PD with the bandwidth of 300 MHz converts the detected probe power into the electric voltage. It is finally sampled and recorded by an oscilloscope (Tektronix, DSA70804) which serves as an ADC with the programmable bandwidth. The optical power before the PD is −5 dBm.

The local pump lightwave is swept nonlinearly, as shown in Fig. 3(b) via a SSBM in Fig. 3(a), and the sweeping range is from 2.33 to 8.33 GHz (corresponding to the gain spectrum from 12 to 18 GHz) with around 4 μs period. Although a DCF is utilized, the dispersion effect can be neglected due to such a narrow optical bandwidth. It can be found that the pump lightwave is swept slower for a higher frequency, which results in a rising $\boldsymbol{H}(\omega)$. The optical spectrum after SSBM is detected by an optical spectral analyzer and given in Fig. 3(c). The lower sideband is selected as the pump lightwave, and the carrier suppression is about 20 dB. To characterize the $\boldsymbol{H}(\omega)$ and ACF, an LFM pulse is first launched into the MZM with the sweeping range from 12 to 18 GHz [see Fig. 3(d)]. After the SBS interaction, the Brillouin gain of the probe lightwave is illustrated in Fig. 3(e). The kinks of the Brillouin gain in Fig. 3(e) are mainly caused by the finite amplitude resolution of the AWG. It can be seen that higher frequency obtains stronger Brillouin gain, which agrees with Eq. (2) and the simulated result shown in Fig. 2(b). The bandwidth of the oscilloscope is set as 200 MHz.

It should be noted that the intensity of $\boldsymbol{H}(\omega)$ in the SBS system not only is dependent on the beat frequency between the pump and probe lightwaves, but also is affected by the microwave signal's power. In order to precisely achieve the IFM, the constructed ACF should be independent on the microwave signal's powers. Here we present a novel method to eliminate the influence of the microwave signal's amplitude. The ACF is relatively constructed by obtaining two independent system responses $\boldsymbol{H}_1(\omega)$ and $\boldsymbol{H}_2(\omega)$ under two different sweeping signals via the AWG [see Fig. 3(a)]. The frequency information can be extracted from these two responses simultaneously, depending on the microwave signal's amplitude. More specifically, we can detect the Brillouin gain of the probe lightwave with a known LFM pulse under two pump lightwaves with different sweeping slopes [see Fig. 3(a)]. Later, we deduce the ratio of two different system responses to be the ACF, i.e., $\mathrm{ACF}(\omega) = \boldsymbol{H}_1(\omega)/\boldsymbol{H}_2(\omega)$.

Figure 4(a) shows two Brillouin gains [$\boldsymbol{H}_1(\omega)$ and $\boldsymbol{H}_2(\omega)$] measured by two different local pump lightwaves (green and blue curves), respectively. The probe lightwave is modulated by a known LFM pulse with its frequency swept from 12 to 18 GHz in 1 μs. The ACF is calculated by $\boldsymbol{H}_1(\omega)/\boldsymbol{H}_2(\omega)$ and plotted in red curve. The sweeping slopes are opposite each other, so that rising and falling responses are obtained and the calculated ACF has a relatively high resolution. Figure 4(b) shows the Brillouin gains of a Costas frequency coded pulse with a 6 GHz bandwidth (from 12 to 18 GHz) and 1 μs duration. There are 10 steps in this coded pulse. Each step lasts for 100 ns, and the frequency gap is 0.6 GHz. Again, two Brillouin gains (D_1 and D_2) are obtained under the two different sweeping slopes. It can be seen that D_1 and D_2 show the opposite variations for these two different pump lightwaves [see the blue and green curves in Fig. 4(b)]. In the same way, we deduce the gain ratio of D_1/D_2. By comparing the ACF [red curve in Fig. 4(a)] and gain ratio of D_1/D_2 [red curves in Fig. 4(b)], the IFM results are evaluated, which are depicted in

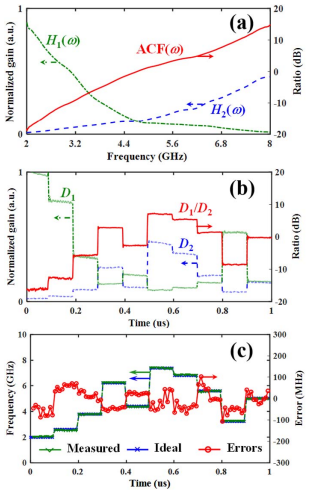

Fig. 4. Measurement results for the frequency Costas coded pulses. (a) Measured ACF, (b) detected Brillouin gain, and (c) measured instantaneous frequency information and the measurement error.

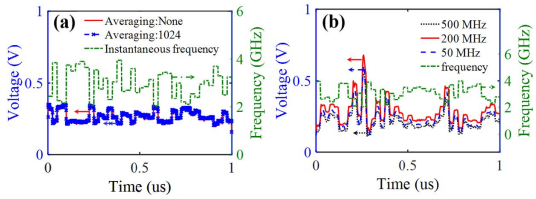

Fig. 5. Comparison of measurement results at C band (a) with and without averaging and (b) with different bandwidths of the ADC.

Fig. 4(c). The measured frequency matches well with the theoretical information, and the errors are within 100 MHz. It should be mentioned that the two different sweeping pump lightwaves are separately applied in two measurements. To potentially achieve a real-time implementation, a parallel configuration to utilize the Brillouin gain and loss effects [21] is now under plan to get D1 and D2, simultaneously.

Two more experiments are carried out to verify the ability of real-time IFM and the requirement of the bandwidth of the PD and ADC. The frequency range of the Costas frequency coded pulse is set from 2 to 4 GHz, and its period is 1 μs. The pulse has totally 40 steps and, thus, its temporal and spectral steps are set as 25 ns and 50 MHz, respectively. As analyzed in Ref. [6], the temporal and spectral resolutions of an SBS-based IFM are at least 10 ns and 50 MHz, respectively. The measured instantaneous frequency information is shown in Fig. 5(a) by a blue curve (with 1024 times averaging) and a red curve (without averaging). Note that the variation of the measurement is opposite the instantaneous frequency information of the Costas frequency coded pulse [green curve in Fig. 5(a)]. This is due to the falling system response being used and, therefore, higher frequency obtains weaker Brillouin gain. It can be seen that the IFM can be achieved without any averaging and, therefore, it is capable for single-shot detection. As discussed above, the ADC bandwidth needed is no more than the width of the BGS, which is about 50 MHz. As compared in Fig. 5(b), the measurement errors for different bandwidths of the OSC are comparable. In consequence, the proposed IFM can be implemented by a PD and/or ADC with a low bandwidth close to the Brillouin linewidth (about 50 MHz).

We have demonstrated an arbitrary-response Brillouin IFM. Instantaneous frequency information of the unknown signal is converted by the principle of frequency-to-power mapping, and the converted information is obtained by detecting the Brillouin gain of the probe lightwave. Through sweeping the frequency of the pump lightwave, the broadband measurement is achieved and the arbitrary response is realized by controlling the frequency sweeping slope of the pump lightwave. Furthermore, we proposed a method with two different sweeping pump lightwaves to measure the microwave signal's frequency without knowing its amplitude information. The 6 GHz instantaneous bandwidth at Ku band has been experimentally achieved with 100 MHz frequency resolution at the cost of ~50 MHz PD and ADC. Note that the Brillouin IFM provides a potential solution for real-time implementation if a parallel configuration is proposed to simultaneously characterize two independent ACF.

Funding. National Natural Science Foundation of China (NSFC) (61822508, 61571292, 61535006).

REFERENCES

1. J. Tsui, *Microwave Receivers with Electronic Warfare Applications* (SciTech, 2005).
2. H. Emami, N. Sarkhosh, L. A. Bui, and A. Mitchell, Opt. Express **16**, 13707 (2008).
3. S. Pan and J. Yao, IEEE Photonicw Technol. Lett. **22**, 1437 (2010).
4. W. Li, N. H. Zhu, and L. X. Wang, IEEE Photonics J. **4**, 427 (2012).
5. H. Jiang, D. Marpaung, M. Pagani, K. Vu, D. Y. Choi, S. J. Madden, L. Yan, and B. J. Eggleton, Optica **3**, 30 (2016).
6. X. Long, W. Zou, and J. Chen, Opt. Express **25**, 2206 (2017).
7. D. Lam, B. W. Buckley, C. K. Lonappan, A. M. Madni, and B. Jalali, IEEE Instrum. Meas. Mag. **18**(2), 26 (2015).
8. H. Gruchala and M. Czyzewski, in *International Conference on Microwave, RADAR, and Wireless Communications (MIKON)* (2004), Vol. **1**, pp. 155–158.
9. J. Tsui and D. L. Sharpin, "Frequency measurement receiver with bandwidth improvement through synchronized phase shifted sampling," U.S. patent 5,198,746 (March30, 1993).
10. J. Niu, S. Fu, K. Xu, J. Zhou, S. Aditya, J. Wu, P. P. Shum, and J. T. Lin, J. Lightwave Technol. **29**, 78 (2011).
11. G. P. Agrawal, *Nonlinear Fiber Optics* (Academic, 2007).
12. B. Vidal, M. A. Piqueras, and J. Marti, Opt. Lett. **32**, 23 (2007).
13. W. Zou, Z. He, and K. Hotate, Opt. Express **17**, 1248 (2009).
14. X. Bao and L. Chen, Sensors **11**, 4152 (2011).
15. K. Y. Song, M. G. Herraez, and L. Thevenaz, Opt. Express **13**, 82 (2005).
16. Z. Zhu, D. J. Gauthier, and R. W. Boyd, Science **318**, 1748 (2007).
17. X. Long, W. Zou, and J. Chen, Opt. Express **24**, 5162 (2016).
18. X. Long, W. Zou, Y. Ji, and J. Chen, Opt. Express **25**, 33330 (2017).
19. A. S. S. Kumar, V. R. Nareddy, A. Mishra, and R. Pant, *Australian Conference on Optical Fibre Technology* (2016), paper AT5C. 5
20. Y. Ji, W. Zou, X. Long, and J. Chen, Opt. Lett. **42**, 2980 (2017).
21. W. Zou, C. Jin, and J. Chen, Appl. Phys. Express **5**, 082503 (2012).